International Journal of Engineering Trends and Technology
ISSN: 2231 – 5381 / https://doi.org/10.14445/22315381/IJETT-V70I4P211

Volume 70 Issue 4, 135-145, April 2022
© 2022 Seventh Sense Research Group®

Original Article

Experimental Investigations of Object based Urban Land Classification of Multispectral IRS R2 Image using Supervised ML Algorithms

Alpesh M. Patel[1], Anil Suthar[2]

[1]*Department of Electronics and Communication, Vishwakarma Government Engineering College, Gujarat Technological University, Ahmedabad, Gujarat, India.*
[2]*New L. J. Institute of Engineering and Technology, Ahmedabad, Gujarat, India.*

[1]am_patel@gtu.edu.in

Received: 22 February 2022 Revised: 30 March 2022 Accepted: 01 April 2022 Published: 26 April 2022

Abstract *- The migration of people towards city and town areas is the dominant factor for urban development and financial policymakers of developing countries like India. In the last decades, numerous availability of satellite data and the increasing computational capability of machines have inspired for effective utilization of remote sensing technology for urban planning. There are various machine learning methods that can be employed for urban land area classification with different performance capabilities. This paper compares six object-based supervised machine learning classifier algorithms with regard to classification accuracy and execution time and investigates the sensitivity of these classifiers for numerous training samples sizes for the classification of the urban area of Surat city. Linear imaging self-scanner (LISS-IV) sensor data of Indian Remote Sensing Resources at-2 (IRS-R2) was utilized for this urban object-based classification (OBC) investigation. The effect of the number of training samples used for training the supervised machine learning classifier has been explored with reference to the kappa coefficient (KC) and overall accuracy (OA) with the Shepherd algorithm used as the segmentation step. The ensemble-based bagging and random forest (RF) algorithms have illustrated superior performance compared to the support vector machine (SVM) classifier for object-oriented classification of urban land. The k neighbors classifier (KNC) has shown the least performance accuracy with an OA of 85.37%. The object-based RF classifier has displayed the highest precision with OA of 93.45% and KC of 0.9 in order to classify an urban area.*

Keywords - *Segmentation, Object-Based Classification (OBC), Machine Learning (ML), Very High Resolution (VHR), Random forest.*

1. Introduction

The classification of earth observation imagery is an important approach of remote sensing technology for distinguishing areas having similar spectral characteristics. In a country like India, urbanization has provided a very good platform for the growth of production, revolution, and business in the infrastructure and service sectors. Millions of people have been employed in this transformation, and there are lots of opportunities in several industries, especially in the information and communication sectors in urban areas. But this migration of people in search of a better quality of life has generated different challenges like overcrowding of people, housing, slums settlements, transportation, waste management, pollution, and environmental challenges for urban planners and management authorities. Remote sensing technology with a rapid and large amount of accessible satellite data can be a convenient and efficient approach to studying the expansion of the urban area. A systematic step-by-step approach is required for the classification of satellite images. The traditional classification methods called pixel-based methods were found effective for low to medium resolution satellite data, where the size of the pixels was comparable with object dimensions, but for very high-resolution satellite images, it is essential to combine the pixels having similar spectral attributes and form the objects [1], [2]. These objects are generated by the segmentation process and utilized in the succeeding processing steps of the object-based classification (OBC) method instead of pixels.

In the last ten years, several machine learning (ML) methods have been used for diverse satellite data classification of various land use applications with pixel-based approach [3]-[5] and object-based method [6]-[10]. D. C. Duro et al. [11] have summarized various studies on comparative analysis of pixel-based classification (PBC) and OBC using a wide range of satellite images and mentioned that OBC method had demonstrated higher perfection in terms of overall categorization accuracy. They have

This is an open access article under the CC BY-NC-ND license (http://creativecommons.org/licenses/by-nc-nd/4.0/)

demonstrated greater classification accuracy for OBC compared to PBC with a support vector machine (SVM), decision tree (DT), and random forest (RF) algorithms for the agriculture landscape. The object-based method has shown meliorated mapping for landslide detection of San Juan La Laguna, Guatemala, compared to pixel-based methods using very high resolution (VHR) satellite data [12]. The nearest neighbor (NN) classifier with fuzzy technique has been used for OBC of wildland-urban interface and shown better results compared to PBC [13]. The comparative analysis of multispectral and pan-sharpened image classification with pixel and object-based approaches using five supervised classifiers was carried out for the agriculture environment using QuickBird satellite image [14]. The object-based method has demonstrated higher perfection in respect of classification precision compared to PBC for all five algorithms and both types of images [14].

B. Fu et al. [15] have inspected the RF algorithm using Gaofen-1 (GF-1), PALSAR, and Radarsat-2 satellite data for pixel and OBC techniques and obtained significant improvement in the accurate measurement for the OBC approach. E. M. O. Silveira et al. [16] have demonstrated OBC modeling as a feasible substitute for a conventional pixel-based method for classification of aboveground biomass of Brazilian forest with higher performance using RF algorithm. The object-based method has shown better results for the classification of Maiella National Park of Italy in terms of overall accuracy (OA) compared to pixel one for 15m panchromatic band of Landsat-8 Operational Land Imager satellite data using random forest machine learning classifier with five spectral indices [17]. Z. Zhou et al. [18] have illustrated higher performance and less salt-and-pepper effects for OBC of WorldView-2 (WV-2) and QuickBird satellite data of coral reef environment of the South China Sea's Spratly Islands in contrast to the pixel-based method. The nearest neighbor (NN) algorithm with an object-based approach has exhibited statistically outstanding higher precision with an overall accuracy of 78.5% compared to the maximum likelihood classifier (MLC) with a pixel-based method with an overall accuracy of 69.5% for land cover mapping of tropical savanna [19]. The object-based image analysis methods are widely employed for change extraction applications for different land types for their higher performance compared to conventional methods for VHR satellite data [20]. The pixel-based DT technique and object-based SVM process were analyzed and compared by Q. Wu et al. [21] for aerial and airborne lidar data. The object-based SVM technique has been found superior, with an overall accuracy of 92.71%, compared to pixel-based DT with an accuracy of 87.77% [21].

The aforementioned studies indicated that the object-based categorization technique is more suitable for VHR satellite image classification compared to pixel one. Numerous studies were performed for comparing various supervised classifiers with object-based methods. The OBC of urban land surface with four ML classifiers C4.5, DT, SVM, RF, and regression tree have been performed by T. Novack et al. [22] on WV-2 image with eight multispectral bands and QuickBird-2 (QB-2) imagery with four spectral bands. The highest accuracy obtained in terms of KC was 0.95 for the RF algorithm and the lowest KC value acquired was 0.57 for the SVM algorithm for this object-based classification [22]. The Multi-scale OBC has been implemented with an object-based RF algorithm with two different earth observation satellite images and attained more than 85% classification accuracy [23]. The comparative examination of object-based SVM, NN, and pixel-level SVM classifier for discriminating salt cedar was executed by L. Xun et al. [24] with QuickBird imagery. The object-based SVM approach has performed better compared to the other two methods, with an OA of 94.6% and a kappa number of 0.93. Y. Qian et al. [25] have analyzed the performance of the classification and regression tree (CART), SVM algorithm, normal Bayes algorithm, and *k* nearest neighbor (KNN) algorithm for OBC of the urban area using (WV-2) satellite imagery. The object-based SVM and NB classifiers have demonstrated superior performance with total accuracy of more than 90% compared to CART and KNN classifiers [25].

D. Li et al. [26] applied object-based SVM and RF classifiers for the urban environment and reported higher performance of SVM for imbalance distribution of training data using WV-2 and WorldView-3 (WV-3) images. The OBC of 0.2 m spatial resolution images of the agricultural environment captured by unmanned aerial vehicles using SVM, RF, DT, and Naive Bayes algorithms were executed by M. Li et al. [27] and concluded that RF and SVM algorithms had shown remarkable higher performance compared to DT and naive Bayes classifiers. B. Melville et al. [28] have analyzed the performance of object-based RF algorithm for recognition of lowland native grassland communities using Landsat ETM+ and WV-2 datasets and achieved OA of 76.72% and 78.26%, respectively. The OBC of high-resolution hyperspectral images of mangrove species acquired using unmanned aerial vehicles has been carried out by J. Cao et al. [29] and reported that SVM has outperformed compared to the KNN algorithm. The SVM and RF classifiers have demonstrated better performance regarding the overall accuracy of OBC of agriculture crop study site compared to KNN and normal Bayes algorithms using multispectral images [30].

The earlier studies have compared various object-based ML classifiers for different land class applications with diverse satellite images. Most of the studies have focused on comparing three to four classification algorithms, and very few were for the urban landscape.

In this paper, six object-based classifiers have been evaluated for their effectiveness and accuracy for the urban area using VHR IRS R2 LISS -IV satellite data.

- In the first part, the performance of six ML classifiers, KNC, SVM, gaussian naive Bayes (GNB), DT, Bagging, and RF, have been investigated for OBC with regard to classification accuracy and execution time using the shepherd algorithm for the segmentation step.
- The second part of the paper demonstrates the sensitivity of these object-based classifiers for various training sample sizes with stratified random sampling techniques.

2. Study Area and Data

For comparative performance investigation of six object-based classification algorithms in an urban area, Surat is chosen as a study region. Surat is a big industrial hub and commercial core of Gujarat. It is also famous for the diamond and cloth manufacturing business. People from all over India come here to work in Diamond manufacturing industry.

Fig. 1 FCC images of the study area

The satellite image of this urban region from the Indian Remote Sensing Satellite, acquired on 19 May 2020, was used as study data. This VHR earth observation image has a spatial resolution of 5m and was captured with LISS-IV (Linear Imaging Self-Scanner) sensors of the Resources at-2 satellite of the Indian Space Research Organisation. The three spectral bands (Red, Green, and NIR) were stacked, and false-colour composites (FCC) image was generated. The subset image from this FCC image with a size of 3716 x 3545 pixels has been utilized for the comparative classification study of the six object-based classifiers. This final FCC image is shown in Fig. 1.

3. Methodology

The comparative study of six ML classifiers for the classification of an urban area with an object-based method has been conducted with a LISS-IV image. The major implementation steps for this comparative performance exploration of object-based methods are mentioned in Fig. 2.

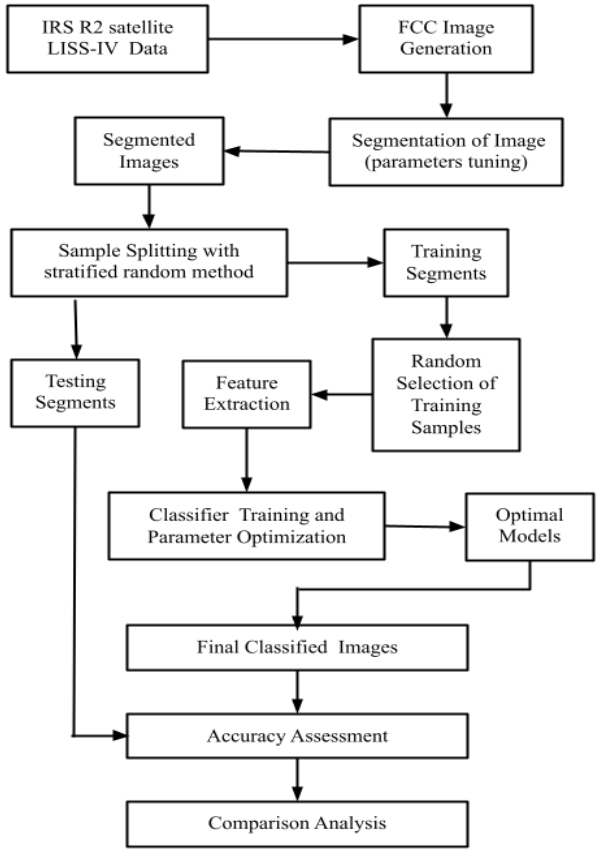

Fig. 2 Workflow of object-based comparative assessment

Three bands of red, green, and NIR of IRS-R2 satellite of LISS-IV sensors were stacked, and the FCC image was created from the multispectral satellite image of an urban area. This FCC image was used to generate proper objects in the segmentation procedure using the shepherd segmentation algorithm as the first important step of OBC. The normalized difference vegetation index (NDVI) image has been constructed and applied as an extracted feature in the classification step. This NDVI image is shown in Fig. 3. The parameters of the segmentation algorithm were tuned to obtain fine segmentation results. The segments from each class have been disassembled in training and examining datasets with the stratified random sampling method. In the next step, features from randomly selected training samples have been extracted and stored for classification function. These extracted features of training samples along with samples were used by the classification algorithm for the separation of input segments into proper classes. For more

accurate results classification algorithm's parameters were optimized with the grid search cross-validation (CV) method. The grid search CV was executed using scikit-learn [31]. The trained optimal models of ML algorithms were used for the classification of segments, and final classified images were obtained. The testing objects were used for the acquisition of accurate statistics of the classified images.

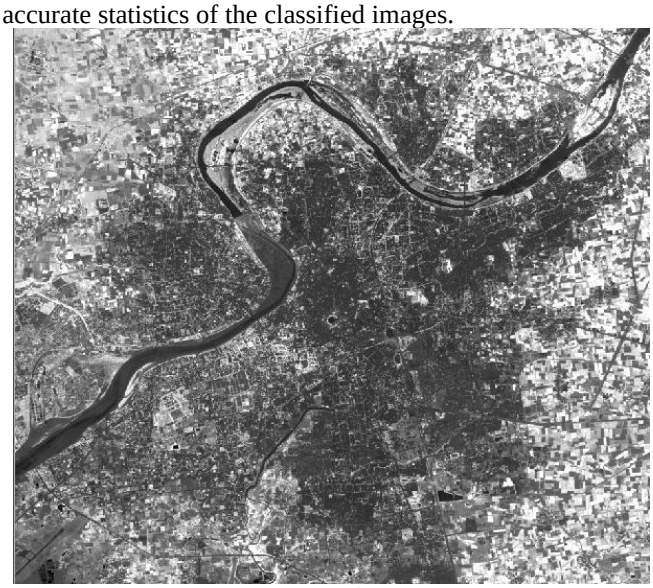

Fig. 3 NDVI image of the study area

3.1 Image Segmentation

This is the initial primary footstep of an object-based method for obtaining meaningful segments by splitting FCC images into spatially contiguous clusters of pixels with close spectral effects [32]. The segments have accumulated details like mean or average numbers from clusters of basic input image bands, and these details are eventually used in the classification of objects [23]. The segmentation inaccuracy because of segmentation as well as over-segmentation makes a major role in the accomplishment of object-based methods for VHR image classification. The under segmentation creates objects having pixels of collective classes, and these multiclass pixels in one segment would be assigned a particular class. Thus errors in the classification are generated [33]. An open-source remote sensing and GIS library (RSGISLib) [34] was used for constructing segments from FCC images with a shepherd segmentation algorithm [35]. A small amount of over-segmentation may incorporate objects of homogeneous classes into one segment [35], [36]. Therefore it was used in the segmentation parameter finalization.

The shepherd algorithm is appropriate for an extensive range of sensors and substantially scalable to a vast area with elementary parameter tuning requirements [35]. In the initial step, seeding using the k-means clustering method is initiated on the image. The unsupervised k-means algorithm had shown preferable performance compared to various clustering algorithms like iterative self-organizing data (OData) and mean-shift [35]. In the next step, pixels are embarked to the relative cluster center, and labeled sectors are created, called clumping. These sectors or groups below minimum size are integrated into spectrally similar and larger size neighbors, and this task is called iterative elimination. It begins with the smallest groups and aims to bring down the number of clumps excessively. After reducing the number of clumps relabeling is performed for confirming sequential arrangements of clumps for systematic classification [35].

The parameter k stipulates the number of initial groups in the k-means assembling action. The other important variable is the size of the clump up to which elimination of small clusters executes [35]. The spectral separation between classes is highly affected by parameter k representing the initial seeds of k-means. The under segmentation and over-segmentation is controlled by the merit of k. The parameter tuning of the shepherd segmentation algorithm for obtaining the best result of segmentation was executed as per [37], [38] with a methodical trial and error approach along with visual examination. The parameters, maximum number of iterations was chosen at 100, and the number of seeds *k* was picked at 60 for this algorithm.

The detailed comparative assessment of this segmentation method has been explored by shepherd et al. using various satellite images with conventional segmentation techniques, for instance, the mean-shift algorithm employed in the Orfeo toolbox, the algorithm of Felzenszwalb and Huttenlocher, multiresolution segmentation technique utilized in recognition software and quick-shift method, and concluded that this segmentation method found dominant in major comparative measures [35].

3.2 Training Samples: Labeling and Selection

The next succeeding step after image segmentation is the assignment of a proper label to each segment that was ended by visual exposition using QGIS software [39]. All the objects of the segmented image have been labeled in one of three classes vegetation, built-up and open land. After class labeling, objects from each class were segregated into training and testing objects. The precision of the classification process can be altered with the number of objects consumed for the training of ML classifiers [40]. At first, out of randomly selected 800 objects of each class, 160 objects per class were kept for testing the performance of ML classifiers, and 640 objects of each class were consumed to train ML classifiers. The effect of the numerous training segments used to train the algorithms of the classifiers was explored for randomly selected 20, 50, 150, 250, 350, 500, and 640 segments from each class.

3.3 Machine Learning Algorithms

The *k* neighbors classifier (KNC) executes learning with *k* nearest neighbors at each node. KNC is a non-parametric [41] and straightforward instance-based machine learning

technique for classification. For a given unknown test segment, it looks at for*k* training segments nearest to test one by applying the distance function. The test segments are labeled based upon the type of the majority of the *k* neighbor segments [42], [43]. The number of neighbors to be considered, weights, and size of the leaf are the parameters tuned for getting the best object-based classification results.

The non-parametric ML algorithm is called a support vector machine (SVM) and perpetrates to detect hyper-plane, which isolates the given data into a fixed amount of classes accordant with given training samples [44]. In binary classification, it allocates class labels from possible two classes to test segments. The prime attribute of the SVM algorithm is that it does not utilize all the training segments for the illustration of splitting hyperplane [44]. SVM is used frequently for satellite image classification because of its potential to operate strongly with compact training data compared to conventional techniques [45]. The regularization parameter *C* and the number of iterations to be executed are the critical variables that have been adjusted for proper classification results.

Gaussian Naive Bayes (GNB) is a parametric and supervised ML algorithm established on Bayes's theorem employing naive conditional independence assumption among pair of features [46]. It approximates covariance matrices and mean vectors for each data type and applies them to assigning correct class labels to input segments [30]. GNB algorithm is ensuing gaussian normal distribution and assists continuous data with a simple and highly scalable approach for classification.

Decision trees (DT) is a non-parametric ML algorithm, and it learns from straightforward rules concluded from features of training data. DT classifies the input data starting with the root node and directs it toward the leaf node. It forms a kind of tree in that branch node constitutes selection from available class and leaf node act for decisions [47]. From numerous DT algorithms like iterative dichotomise 3 (ID3), C4.5, C5.0, and CART, for object-based classification of this urban VHR data, the CART algorithm has been implemented using [31]. The Gini index computes the separation between possibilities scattering of sample features [47] and is considered as a node cleaving criteria to structure a tree. The highest extent of the tree and the kind of attributes required to be examined for node split were the prime parameters used in optimization to obtain the finest classification result.

The ensemble technique integrates the outputs of various base classifiers to increase the fitness compared to a single estimator. In bagging classifiers, various random subsets of training data are used to construct the numerous instances of a base estimator, and their independent results are aggregated to provide a final accurate prediction. By creating randomness in bagging algorithm construction, the variance of the base classifier is reduced, and it makes the algorithm superior to a single base estimator [31]. In the implemented bagging method, a random subset of training data sets was drawn with replacement. The prime parameters considered as optimization parameters of the bagging classifier were the number of base classifiers and the number of characteristics to figure out the subset of the dataset.

A random forest (RF) algorithm may be represented as an ensemble of weak classifiers like DT, where each DT provides a single vote, and the class having the most repeated answer is assigned to the input segment [48]. This ML classifier method was found by [49], and here, trees are combined with the replacement of a random subset, and attributes are also randomly picked out for the best division of each node. This ensemble technique has operated well with large dimensional data and evaluated the gravity of variables in the classification task [50]. The number stating the trees in the forest, amounts of attributes to examine for node splitting, and extreme depth of the tree was inspected as the foremost parameters for optimization of the RF classifier using [31].

3.4 Validation and Accuracy Assessment

The generalization errors are evaluated by applying k-fold cross-validation (CV). Here, in the model validation technique, *k* subsets are prepared from available training segments, and the *k*-1 subsets are utilized for training the ML algorithm. Then the evolving trained model is authenticated on a residual subspace of training data [48]. The performance precision of CV is generated by calculating the average accuracy in the loop. Here parameter optimization of ML classifiers was accomplished by executing a 5-fold CV using the grid search CV module of [31].

The overall or total classification accuracy is deliberated as a fraction of truly classified pixels and an entire number of pixels [51]. The division of rightly categorized pixels of a certain group and all the pixels of that class in reference data is considered as producer's accuracy (PA) or error of omission [48], [51]. The fraction of accurately classified pixels of a category and the summations of pixels categorized in this class is observed as user's accuracy (UA) or commission error [48], [51]. The measurement of Cohen's [52] kappa coefficient (KC) using observed agreement (OA) and expected agreement (percentage of pixels observed correctly by chance) is elaborated by [53].

4. Results and Discussion

The VHR image of the IRS R2 satellite of Surat with 5m spatial resolution has been subdivided with the help of the shepherd segmentation algorithm and classified with six ML classifiers through an object-based approach.

Table 1. Precision comparison of KNC, SVM, GNB, DT, Bagging, and RF Classifiers

Classes	KNC		SVM		GNB		DT		Bagging		RF	
	UA	PA	UA	PA	UA	PA	UA	PA	UA	PA	UA	PA
Vegetation	0.88	0.95	0.88	0.97	0.97	0.96	0.96	0.97	0.96	0.97	0.96	0.97
Open land	0.97	0.73	0.88	0.85	0.83	0.94	0.96	0.87	0.96	0.89	0.97	0.89
Built-up	0.69	0.97	0.81	0.75	0.87	0.62	0.79	0.94	0.82	0.94	0.83	0.97
OA	85.37		86.55		87.85		91.53		92.59		93.45	
KC	0.78		0.79		0.80		0.87		0.88		0.90	
ET	45.60		127.01		29.56		33.03		37.76		461.69	

Table 2. Comparison of OA (%) of KNC, SVM, GNB, DT, Bagging, and RF Classifiers for different TS per class

Classifiers	Number of Training Samples (TS)						
	20	50	150	250	350	500	640
RF	87.67	88.25	89.26	91.69	92.19	92.59	93.45
Bagging	85.55	86.24	88.33	89.80	90.29	91.79	92.59
DT	83.48	85.53	86.06	87.99	88.83	89.40	91.53
GNB	83.59	86.83	87.75	87.80	87.82	88.01	87.85
SVM	74.77	80.53	82.26	82.70	86.31	86.68	86.55
KNC	80.93	83.77	84.70	84.65	84.93	85.35	85.37

Table 3. Comparison of KC of KNC, SVM, GNB, DT, Bagging, and RF Classifiers for different TS per class

Classifiers	Number of Training Samples (TS)						
	20	50	150	250	350	500	640
RF	0.81	0.82	0.83	0.87	0.88	0.89	0.90
Bagging	0.78	0.79	0.82	0.84	0.85	0.87	0.88
DT	0.75	0.78	0.79	0.81	0.83	0.84	0.87
GNB	0.73	0.79	0.80	0.80	0.80	0.81	0.80
SVM	0.60	0.69	0.71	0.74	0.78	0.79	0.79
KNC	0.70	0.75	0.77	0.77	0.77	0.78	0.78

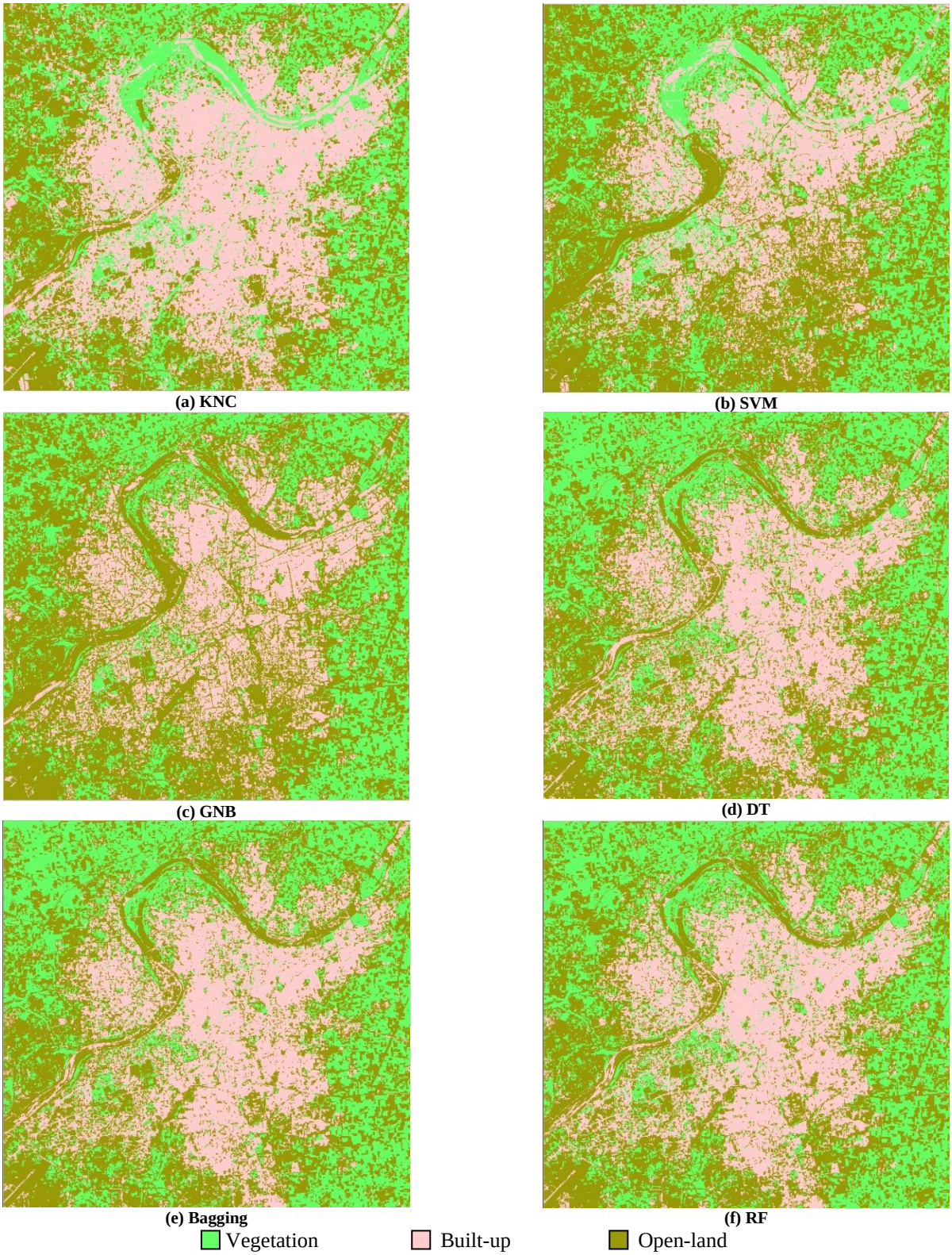

Fig. 4 Classified images of (a) KNC, (b) SVM, (c) GNB, (d) DT, (e) Bagging, and (f) RF Classifiers

This VHR image was classified into three categories such as vegetation, open land, and built-up. The performance achievement of KNC, SVM, GNB, DT, bagging, and RF machine learning classifiers for urban study areas has been indicated in Table I. The stratified random sampling procedure was employed for differentiating the output of the shepherd segmentation algorithm into training and verification segments. 640 segments from all groups have been applied for the training of ML classifiers, and 160 samples per class have been examined as test samples precision calculation. The various performance quantification like OA, user's accuracy (UA), producer's accuracy (PA), and KC are calculated for the aforementioned six object-based classifiers and demonstrated in Table 1.

The built-up class demonstrates the urban development of the city area, and the vegetation class shows the effect of urbanization on the natural environment of a city area. The object-based DT has illustrated better OA and KC compared to KNC, SVM, and GNB classifiers. The execution time - ET is measured in seconds by taking an average of 10 executions of object-based classification for each ML classifier and shown in Table - I. The ensemble-based bagging and RF classifiers have indicated higher classification accuracy with regard to OA and KC. The execution time of the RF algorithm was found to be worst compared to all other classifiers, but it has shown the highest OA of 93.45% and KC of 0.90. The computation time of the DT classifier was found less compared to KNC and bagging algorithms. In the matter of class-wise UA and PA, the vegetation class has performed better for all six algorithms. GNB classifier has indicated greater accuracy with OA of 87.85% and KC of 0.80, and it has shown better computation time compared to the SVM algorithm. The computation time of DT was noticed much less compared to SVM and RF classifiers. The ensemble-based bagging classifier has achieved a much lower execution time compared to RF, with precision statistics near to that of the RF classifier.

The final classified output image of KNC, SVM, GNB, DT, bagging, and RF machine learning algorithms for urban study areas are illustrated in Fig. 4. In the object-based classified images, the built-up class was shown in light pink color, vegetation area was represented in light green color, and open land area was illustrated in light brown color. The misclassification of the built-up class for the classified image of the KNC algorithm can be noticed more compared to other classified images. A remarkable advancement in the classified images of DT, bagging, and RF classifiers can be envisioned compared to classified images of KNC, SVM, and GNB classifiers.

The sensitivity of KNC, SVM, GNB, DT, bagging, and RF machine learning classifiers was assessed using 20, 50, 150, 250, 350, 500, and 640 randomly picked training samples (TS). The overall accuracy of these object-based classifiers with above mentioned randomly selected TS is shown in Table 2, and kappa statistics are mentioned in Table 3. The general observation can be stated that as the number of training segments is raised, the final categorization accuracy with regard to OA and KC is also raised for all the six classifiers. The increase in values of OA and KC can be observed higher for the initial columns of Table 2 and Table 3, and then the rise in the accuracy value is observed less.

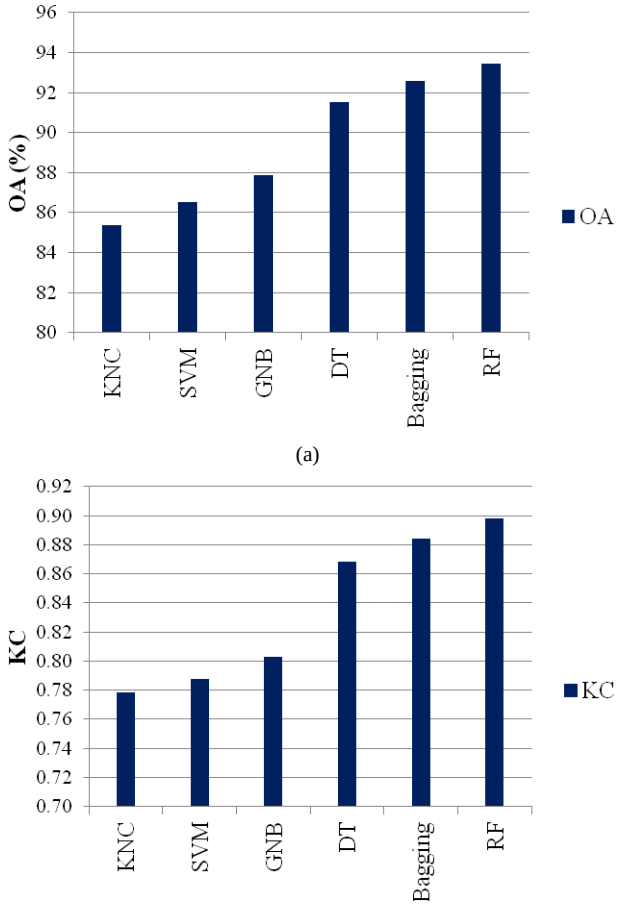

Fig. 5 (a) overall accuracy and (b) kappa coefficient of KNC, SVM, GNB, DT, Bagging, and RF Classifiers

Fig. 5 (a) and (b) display the accuracy of the classification of urban land obtained by KNC, SVM, GNB, DT, bagging, and RF machine learning classifiers in respect of OA and KC. The graph of OA and KC against 20, 50, 150, 250, 350, 500, and 640 randomly picked training samples for object-based KNC, SVM, and GNB classifiers are illustrated in Fig. 6 (a) and (b). From these figures, it can be stated that GNB has demonstrated better performance with regard to both OA and KC compared to KNC and SVM algorithms for all the training samples. As the amount of training samples decreases, the precision of the SVM classifier reduces more compared to the other two classifiers. Fig. 7 (a) and (b) exhibit the variation in OA and KC of DT, bagging, and RF

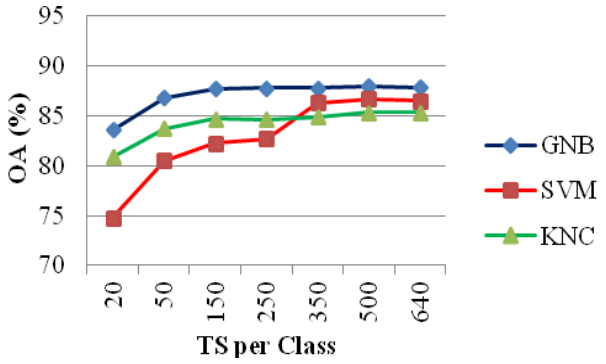

(a)

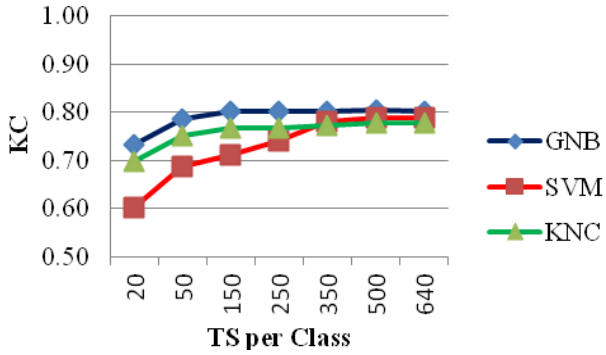

(b)

Fig. 6 (a) overall accuracy and (b) kappa coefficient of KNC, SVM, and GNB classifiers for different TS per class

Machine-learning classifiers for various randomly chosen training samples. From these line charts, OA and KC have been observed to be superior for RF classifiers compared to DT and bagging algorithms for all the training sample sizes.

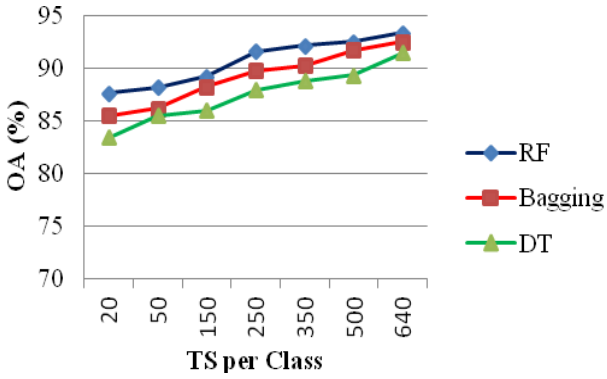

(a)

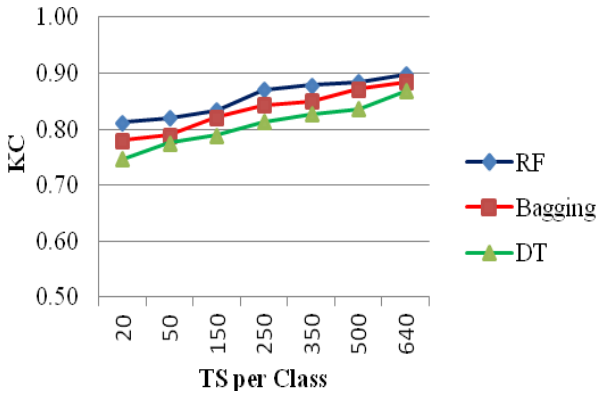

(b)

Fig. 7 (a) overall accuracy and (b) kappa coefficient of DT, bagging, and RF classifiers for different TS per class

Accuracy measurements OA and KC for DT classifier have been seen as smaller compared to ensemble-based bagging and RF algorithms.

The different accuracy statistics and comparison of six ML classifiers for classification of an urban area with 20, 50, 150, 250, 350, 500, and 640 randomly selected TS have been mentioned in Tables I to III. The object-based RF algorithm has outperformed compared to the other five classifiers with regard to OA and KC for varied training segment numbers.

5. Conclusion

In the last few decades, a rapid increase in urbanization has been observed in developing countries such as India. The remote sensing technology with innumerable satellite data can be used effectively for urban planning and development. In this paper, KNC, SVM, GNB, DT, bagging, and RF machine learning classifiers were elaborated for urban land classification using the efficient object-based classification (OBC) method. The performance of these six supervised classifiers has been demonstrated and compared concerning overall accuracy (OA), kappa coefficient (KC), and execution time (ET) using LISS -IV very high-resolution multispectral data from the IRS R-2 satellite. A shepherd algorithm was used as a segmentation step in the object-based urban landscape classification. The ensemble type bagging and RF algorithms have shown the best performance for OBC, with OA of 92.59% and 93.45%, respectively. In terms of execution time, the object-based DT classifier has performed better compared to bagging and RF classifiers.

The sensitivity of these machine learning algorithms has been analyzed with various training sample sizes, and the RF classifier has performed better in this investigation. From this sensitivity analysis, it is observed that the accomplishment of these six machine learning classifiers with regard to OA and

KC increases with an escalation in the number of training segments. The GNB classifier has demonstrated the best results in terms of computation time compared to all six machine learning algorithms.

Acknowledgment

We gratefully acknowledge the Space Applications Centre (SAC) of the Indian Space Research Organisation (ISRO), Ahmedabad, India, for giving IRS LISS-IV multispectral image.

References

[1] T. Blaschke, Object-based image analysis for remote sensing, ISPRS J. Photogramm. Remote Sens. vol. 65(1) (2010) 2–16.
[2] R. C. Estoque, Y. Murayama, and C. M. Akiyama, Pixel-based and object-based classifications using high- and medium-spatial-resolution imageries in the urban and suburban landscapes, Geocarto Int. 30(10) (2015) 1113–1129.
[3] N. Zhang, Y. Wu, and Q. Zhang, Detection of sea ice in sediment-laden water using MODIS in the Bohai Sea: a CART decision tree method, Int. J. Remote Sens. 36(6) (2015) 1661–1674.
[4] E. Raczko and B. Zagajewski, Comparison of support vector machine, random forest and neural network classifiers for tree species classification on airborne hyperspectral APEX images, Eur. J. Remote Sens. 50(1) (2017) 144–154.
[5] P. Thanh Noi and M. Kappas, Comparison of Random Forest, k-Nearest Neighbor, and Support Vector Machine Classifiers for Land Cover Classification Using Sentinel-2 Imagery, Sensors (Basel). 18(1) (2017)
[6] L. Ballantine, L. Blasius, E. Hines, and B. Kruse, Tree species classification using hyperspectral imagery: A comparison of two classifiers, Remote Sens. 8(6) (2016) 1–18.
[7] S. Amini, S. Homayouni, A. Safari, and A. A. Darvishsefat, Object-based classification of hyperspectral data using Random Forest algorithm, Geo-Spatial Inf. Sci. 21(2) (2018) 127–138.
[8] Y. Cai, H. Lin, and M. Zhang, Mapping paddy rice by the object-based random forest method using time series Sentinel-1/Sentinel-2 data, Adv. Sp. Res. 64(11) (2019) 2233–2244.
[9] Z. Shirvani, A holistic analysis for landslide susceptibility mapping applying geographic object-based random forest: A comparison between protected and non-protected forests, Remote Sens. 12(3) (2020) 1–22.
[10] Harmony, V. P. Siregar, S. Wouthuyzen, and S. B. Agus, Object-based classification of benthic habitat using Sentinel 2 imagery by applying with support vector machine and random forest algorithms in shallow waters of Kepulauan Seribu, Indonesia, Biodiversitas. 23(1) (2022) 514–520.
[11] D. C. Duro, S. E. Franklin, and M. G. Dubé, A comparison of pixel-based and object-based image analysis with selected machine learning algorithms for the classification of agricultural landscapes using SPOT-5 HRG imagery, Remote Sens. Environ. 118(2012) 259–272.
[12] R. N. Keyport, T. Oommen, T. R. Martha, K. S. Sajinkumar, and J. S. Gierke, A comparative analysis of pixel- and object-based detection of landslides from very high-resolution images, Int. J. Appl. Earth Obs. Geoinf. 64 (2018) 1–11.
[13] C. Cleve, M. Kelly, F. R. Kearns, and M. Moritz, Classification of the wildland-urban interface: A comparison of pixel- and object-based classifications using high-resolution aerial photography, Comput. Environ. Urban Syst. 32(4) (2008) 317–326.
[14] I. L. Castillejo-González et al., Object- and pixel-based analysis for mapping crops and their agro-environmental associated measures using QuickBird imagery, Comput. Electron. Agric. 68(2) (2009) 207–215.
[15] B. Fu et al., Comparison of object-based and pixel-based Random Forest algorithm for wetland vegetation mapping using high spatial resolution GF-1 and SAR data, Ecol. Indic. 73 (2017) 105–117.
[16] E. M. O. Silveira et al., Object-based random forest modelling of aboveground forest biomass outperforms a pixel-based approach in a heterogeneous and mountain tropical environment, Int. J. Appl. Earth Obs. Geoinf. 78 (2019) 175–188.
[17] A. Tassi, D. Gigante, G. Modica, L. Di Martino, and M. Vizzari, Pixel-vs. Object-based Landsat 8 data classification in google earth engine using random forest: The case study of Majella national park, Remote Sens. 13(12) (2021) 2299.
[18] Z. Zhou, L. Ma, T. Fu, G. Zhang, M. Yao, and M. Li, Change detection in coral reef environment using high-resolution images: Comparison of object-based and pixel-based paradigms, ISPRS Int. J. Geo-Information. 7(11) (2018) 441.
[19] T. G. Whiteside, G. S. Boggs, and S. W. Maier Comparing object-based and pixel-based classifications for mapping savannas, Int. J. Appl. Earth Obs. Geoinf. 13(6) (2011) 884–893.
[20] M. Hussain, D. Chen, A. Cheng, H. Wei, and D. Stanley, ISPRS Journal of Photogrammetry and Remote Sensing Change detection from remotely sensed images : From pixel-based to object-based approaches, ISPRS J. Photogramm. Remote Sens. 80 (2013) 91–106.
[21] Q. Wu, R. Zhong, W. Zhao, H. Fu, and K. Song, A comparison of pixel-based decision tree an object-based support vector machine methods for land-cover classification based on aerial images and airborne lidar data, Int. J. Remote Sens. 38(23) (2017) 7170–7195.
[22] T. Novack, T. Esch, H. Kux, and U. Stilla, Machine learning comparison between WorldView-2 and QuickBird-2-simulated imagery regarding object-based urban land cover classification, Remote Sens. 3(10) (2011) 2263–2282.
[23] D. C. Duro, S. E. Franklin, and M. G. Dubé, Multi-scale object-based image analysis and feature selection of multi-sensor earth observation imagery using random forests, Int. J. Remote Sens., 33(14) (2012) 4502–4526.
[24] L. Xun and L. Wang, An object-based SVM method is incorporating optimal segmentation scale estimation using Bhattacharyya Distance for mapping salt cedar (Tamarisk spp.) with QuickBird imagery, GIScience Remote Sens. 52(3) (2015) 257–273.
[25] Y. Qian, W. Zhou, J. Yan, W. Li, and L. Han, Comparing machine learning classifiers for object-based land cover classification using very high-resolution imagery, Remote Sens. 7(1) (2015) 153–168.
[26] D. Li, Y. Ke, H. Gong, and X. Li, Object-based urban tree species classification using bi-temporal worldview-2 and worldview-3 images, Remote Sens. 7(12) (2015) 16917–16937.

[27] M. Li, L. Ma, T. Blaschke, L. Cheng, and D. Tiede, A systematic comparison of different object-based classification techniques using high spatial resolution imagery in agricultural environments, Int. J. Appl. Earth Obs. Geoinf. 49 (2016) 87–98.
[28] B. Melville, A. Lucieer, and J. Aryal, Object-based random forest classification of Landsat ETM+ and WorldView-2 satellite imagery for mapping lowland native grassland communities in Tasmania, Australia, Int. J. Appl. Earth Obs. Geoinf. 66 (2018) 46–55.
[29] J. Cao, W. Leng, K. Liu, L. Liu, Z. He, and Y. Zhu, Object-Based mangrove species classification using unmanned aerial vehicle hyperspectral images and digital surface models, Remote Sens. 10(1) (2018) 89.
[30] G. Modica, G. De Luca, G. Messina, and S. Praticò, Comparison and assessment of different object-based classifications using machine learning algorithms and UAVs multispectral imagery: a case study in a citrus orchard and an onion crop, Eur. J. Remote Sens. 54(1) (2021) 431–460.
[31] Pedregosa et al., Scikit-learn: Machine Learning in Python, Journal of Machine Learning Research. 12 (2011) 2825-2830.
[32] T. Blaschke et al., Geographic object-based image analysis towards a new paradigm, ISPRS J. Photogrammetry Remote Sens. 87 (2014) 180–191.
[33] D. Liu and F. Xia, Assessing object-based classification: Advantages and limitations, Remote Sens. Lett. 1(4) (2010) 187–194.
[34] D. Clewley et al., A python-based open-source system for Geographic Object-Based Image Analysis (GEOBIA) utilizing raster attribute tables, Remote Sens. 6(7) (2014) 6111–6135.
[35] J. D. Shepherd and P. Bunting, Operational Large-Scale Segmentation of Imagery Based on Iterative Elimination, Remote Sens. 11(6) (2019) 658.
[36] Career, A.P.; Debeir, O.; Wolff, E., Assessment of Very High Spatial Resolution Satellite Image Segmentations, Photogramm. Eng. Remote Sens. 71(11) (2005) 1285-1294.
[37] R. Mathieu and J. Aryal, Object-based classification of Ikonos imagery for mapping large-scale vegetation communities in urban areas, Sensors, 7(11) (2007) 2860–2880.
[38] M. A. Aguilar, M. M. Saldana, and F. J. Aguilar, GeoEye-1 and WorldView-2 pan-sharpened imagery for object-based classification in urban environments, Int. J. Remote Sens. 34(7) (2013) 2583–2606.
[39] QGIS Development Team, QGIS (Version 2.18). Open Source Geospatial Foundation Project. (2019) https://qgis.org/en/site/.
[40] P. Du, A. Samat, B. Waske, S. Liu, and Z. Li, Random Forest and Rotation Forest for fully polarized SAR image classification using polarimetric and spatial features, ISPRS J. Photogramm. Remote Sens. 105 (2015) 38–53.
[41] Duda, Richard O. and Peter E. Hart. Pattern classification and scene analysis. A Wiley-Interscience Publication. 3 (1973) 731-739.
[42] Akbulut, Yaman, Abdulkadir Sengur, Yanhui Guo, and Florentin Smarandache. NS-k-NN: Neutrosophic set-based k-nearest neighbors classifier, Symmetry 9(9) (2017) 179.
[43] Wei, Chuanwen, et al. Estimation and mapping of winter oilseed rape LAI from high spatial resolution satellite data based on a hybrid method, Remote Sensing. 9(5) (2017) 488.
[44] Mountrakis, G.; Im, J.; Ogle, C. Support vector machines in remote sensing: A review, ISPRS J. Photogramm. Remote Sens. 66(3) (2011) 247–259.
[45] Mantero, Paolo, Gabriele Moser, and Sebastiano B. Serpico. Partially supervised classification of remote sensing images through SVM-based probability density estimation, IEEE Transactions on Geoscience and Remote Sensing 43(3) (2005) 559-570.
[46] K. Liakos, P. Busato, D. Moshou, S. Pearson, and D. Bochtis, Machine Learning in Agriculture: A Review, Sensors. 18(8) (2018) 2674.
[47] S. Singh and P. Gupta, Comparative Study Id3, Cart and C4.5 Decision Tree Algorithm: a Survey, Int. J. Adv. Inf. Sci. Technol. 27(27) (2014) 97–102.
[48] L. Sun and K. Schulz, The Improvement of Land Cover Classification by Thermal Remote Sensing, Remote Sensing, 7(7) (2015) 8368–8390.
[49] L. Breiman, Random forests, Machine learning 45(1) (2001) 5-32.
[50] Rodriguez-Galiano, Victor Francisco, et al., An assessment of the effectiveness of a random forest classifier for land-cover classification, ISPRS journal of photogrammetry and remote sensing. 67 (2012) 93-104.
[51] The story, Michael, and Russell G. Congalton, Accuracy assessment: a user's perspective, Photogrammetric Engineering and remote sensing. 52(3) (1986) 397-399.
[52] Cohen, Jacob, A coefficient of agreement for nominal scales, Educational and psychological measurement. 20(1) (1960) 37-46.
[53] Gómez, Daniel, and Javier Montero Determining the accuracy in image supervised classification problems, (2011) 342-349.